Proceedings of the 8th International Conference on Applied Informatics
Eger, Hungary, January 27–30, 2010. Vol. 1. pp. 175–184.

Automatic Detection of the Fovea and Optic Disk in Digital Retinal Images by Combining Algorithms*

Rashid Jalal Qureshi, Laszlo Kovacs, Brigitta Nagy
Balazs Harangi, Andras Hajdu

Faculty of Informatics, University of Debrecen, POB 12, Debrecen, H-4010, Hungary
e-mail: {rashid.jalal, hajdu.andras}@inf.unideb.hu

Abstract

Diabetic retinopathy (DR) is the damage to the eye's retina that occurs with long-term diabetes, which can eventually lead to blindness. Screening programs for DR are being introduced, however, an important prerequisite for automation is the accurate location of the main anatomical features in the image, notably the optic disc (OD) and the macula. A series of interesting algorithms have been proposed in the recent past and the performance is generally good, but each method has situations, where it fails. This paper presents a combining framework for automatic detection of optic disc and macula in retinal fundus images using a combination of different optic disc and macula detectors. The extensive tests have shown that combining the detectors is more accurate than any of the individual detectors making up the ensemble.

Keywords: Biomedical image processing, Diabetic retinopathy, Macula detection, Optic disc detection, Retinal imaging, Medical decision making.

1. Introduction

Diabetic retinopathy (DR) is commonest cause of blindness in the working-age population in developed countries. Screening programs for DR are being introduced and automation of image grading would have a number of benefits. However, an important prerequisite for automation is the accurate location of the main anatomical features in the image (Figure 1), notably the optic disc and the macula. The

*This work was supported in part by the Janos Bolyai grant of the Hungarian Academy of Sciences, and by the TECH08-2 project DRSCREEN- Developing a computer based image processing system for diabetic retinopathy screening of the National Office for Research and Technology of Hungary (contract no.: OM-00194/2008, OM-00195/2008, OM-00196/2008).

optic disk is a circular shaped anatomical structure with a bright appearance. The fovea is the very center of the macula, the site of our sharpest vision. The locations of these features are necessary because the severity and characterization of abnormalities in the eye partially depends on its distance to the fovea. In most of the techniques presented in the recent past [1-3], there is a two-step strategy, i.e., prior to the macula detection, the optic disk size and position is computed. Then, following the morphological properties of the eye, the macula location and size is determined. For example, in [4] morphological filtering and active contours are used to find the boundary of the optic disc, while in [5] morphological operations are combined with Hough transform to localize OD.

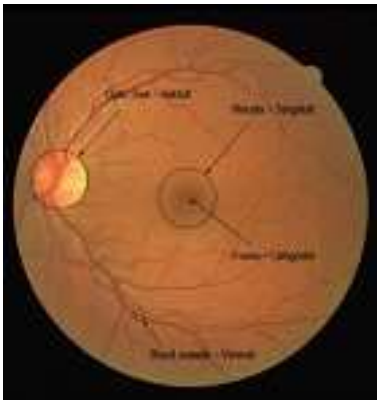

Figure 1: A retinal fundus images and main anatomical parts.

There is in fact no reason to assume that a single algorithm would be optimal for macula or OD center detection. It is more likely that different methods have complementary strengths and combining different detectors together in a systems can substantially improve the overall performance. In the proposed approach, we have combined the outputs of five optic disc and five macula detectors. The criteria for the selection of the candidate algorithms to be combined is based on their precise detection performance and low computation time. The results shows that the proposed method has achieved highest performance.

2. Algorithms used for the proposed graph based system

In this section we present some state-of-the-art OD and macula detectors that were selected for the proposed combination scheme. These algorithms were implemented to return the macula and OD center as a single pixel.

2.1. Description of algorithms used for detecting optic disc

2.1.1. Based on pyramidal decomposition ($\mathbf{OD}_{pd}$)

Based on the hypothesis that the optic disc is roughly a circular patch of bright pixels surrounded by darker pixels Lalonde *et al.* [6] propose to locate the candidate OD regions on the green plane of the original image by mean of pyramidal decomposition (Haar-based discrete wavelet transform). In the low resolution image, pixels which have the highest intensity values compared to the mean pixel intensity over the search area were selected as possible candidates. Next, smoothing is done within each of these regions and the brightest pixel is selected as a possible OD center point. Its confidence value is computed as the ratio of average pixel intensity inside a circular region centered at the brightest pixel and the average intensity in its neighborhood.

2.1.2. Based on edge detection ($\mathbf{OD}_{ed}$)

In this method, Lalonde *et al.* [6] search the area identified by the pyramidal decomposition (see section 2.1.1) for a circular shape. To reduce the number of regions of interest, contiguous regions were aggregated into a single zone. A binary edge map is obtained by performing Canny edge detection in the region of interest first, and then a thresholded image I_T is obtained with a special threshold value computed from noisy edge map. The search for the OD contour is performed using an algorithm based on Hausdorff distance that provide a degree of mismatch between two sets of points. Hence, a percentage of matches are computed, and if the certain proportion of the pixels template is found to overlap edge pixels in $I_T$then the location is retained as the centre point of a potential OD candidate.

2.1.3. Based on entropy filter ($\mathbf{OD}_{ef}$)

Sopharak *et al.* [7] presented the idea of detecting the OD by entropy filtering. The original RGB image is transformed into HSI color space, median filtering is applied to remove possible noise and for contrast enhancement contrast limited adaptive histogram equalization (CLAHE) is done to the I band. After preprocessing, optic disc detection is performed by probability filtering. Binarization is done with Otsu's algorithm [8] to separate the complex regions from the smooth ones, and the largest connected region with an approximately circular shape is marked as a candidate for the OD.

2.1.4. Based on Hough transformation ($\mathbf{OD}_{ht}$)

Ravishankar *et al.* [9] tried to track the OD by combining the convergence of the only thicker blood vessel initiating from it and high disk intensity properties in a cost function. On initially resized image to standard resolution (768×576), a grayscale closing operation is performed on the green channel image. This step is followed by thresholding and median filtering to obtain the binary image of the

blood vessels. The segments of the thicker blood vessels skeleton are modeled as lines found by the Hough transform. The dataset of lines generated is reduced by removing those lines with slopes $\theta < 45^0$. This reduced dataset of lines is intersected pair- wise to generate an intersection map. The map is dilated to make the region of convergence more apparent. A weighted image is produced by combining this dilated intersection map and preprocessed green channel image. A cost function is defined to obtain the optimal location of the OD that is a point which maximizes the cost function.

2.1.5. Based on feature vector and uniform sample grid ($\mathbf{OD}_{fv}$)

Niemeijer *et al.* [10] defines a set of features based on vessel map and image intensity, measured under and around a circular template to determine the location of the OD. Each image is scaled so that the width of its field of view (FOV) is 630 pixels. The binary vessel map obtained [11] is thinned and all the centerline pixels that have two or more neighbors are removed. Next, the orientation of the vessels is measured by applying principal component analysis on each centerline pixel with its neighboring pixel on both sides. A two step sampling process is launched to get the training database. First, using the circular template of radius $r = 40$ pixels having manually selected OD center within the radius, all features are extracted for each sample location (a uniform grid spaced 8 pixels apart) of the template including distance d to the true center. In the second step, 500 randomly selected location (i.e., not on a grid) in the training image were sampled in a similar fashion. To locate the OD, a sample grid (grid points spaced 10 pixels apart) is overlaid on top of the complete FOV and features vector are extracted and rough location of OD is found containing pixels having lowest value of d. The process is repeated with a 5x5 pixel grid centered on the rough OD location to get the more accurate OD center.

2.2. Description of algorithms used for detecting macula

2.2.1. Macula detection based on intensity ($\mathbf{M}_I$)

In [12] a region of interest (ROI) is defined to process macula detection. A Gaussian low pass filter is applied to smooth the intensity of the image. The statistical mean and standard deviation of the ROI area is used to compute a threshold for segmentation to get binary objects. The object that is located nearest to the center of the ROI is labeled as macula. Its center of mass is considered to be the center of the macula. However, we did some modification to this approach, because it is not mentioned how this ROI is defined; therefore we applied the smoothing to the whole image using a large kernel (70×70 pixels with $\sigma = 10$) so that vascular network and small patches do not interfere in detection. Then, an iterative thresholding process is launched to generate a set of binary images corresponding to different threshold values. In each binary image, the object satisfying the area and distance from the center constraints are identified, and the object found nearest to the center

with minimum surface area is marked as macula.

2.2.2. Macula detection based on spatial relationship with the optic disc ($\mathbf{M}_{sr}$)

In [3] a region of interest (ROI) for macula is defined by means of its spatial relationship with the OD. That is the portion of a sector subtended at the center of the optic disk by an angle of 30ş above and below the line between this center and the center of the retinal image disk. The macula is identified within this ROI by iteratively applying a threshold, and then applying morphological opening (erosion followed by dilation) on the resulting blob. The value of the threshold is selected such that the area of the smoothed macula region is not more than 80% of that of the detected optic disk. The fovea is simply determined as the centroid of this blob.

2.2.3. Macula detection based on temporal arcade ($\mathbf{M}_{ta}$)

Fleming et al. [1] proposed to identify the macular region based on the information of the temporal arcade and OD center. First, the arcade was found by using semielliptical templates. Next, the optic disc was detected by using a Hough transform with circular templates having diameters from 0.7 to 1.25 OD diameter (DD). Finally, the fovea was detected by finding the maximum correlation coefficient between the image and a foveal model. The search was restricted to a circular region with diameter 1.6 DD centered on a point that is 2.4 DD from the optic disc and on a line between the detected optic disc and the center of the semi-ellipse fitted to the temporal arcades.

2.2.4. Macula detection based on Watershed and morphological operators ($\mathbf{M}_{wm}$)

Zana et al. [13] presented a region merging algorithm based on watershed cell decomposition and on morphological treatments for macula recognition. After noise removal, morphological closing followed by opening is performed to remove the small dark holes and white spots. A watershed based decomposition of the gradient image into cells is done, and the cell with darkest gray level inside the macula is selected as the first step of a merging algorithm. A complex criterion based on the gray values and of edges of the filtered image is calculated to merge the cells of the macula while rejecting perifoveal inter-capillary zones in order to produce the contour of the macula.

2.2.5. A novel approach ($\mathbf{M}_{n}$)

Besides the algorithms discussed so far, we have also tested our novel contribution for macula detection and used its results in our combined system. First, we extract the green plane form the color fundus image. We generate the background image by applying median filter and subtract it from the green plane, resulting in a shade

corrected image. Next, we binarize the image by considering all-non zero pixels as foreground pixels, and others as background. Finally, we apply an image labeling procedure and select the largest component as the macula.

3. Proposed combination of the algorithms

As discussed in [14], an ensemble classifier can be more accurate than any of its individual members if the individual classifiers are doing better than random guessing. Because, if the algorithms are complementary, then when one or a few algorithm makes an error, the probability is high that the remaining algorithms can correct this error.

3.1. Computing distribution shift factors

The macula/OD centers detected by a particular algorithm in all test images are mapped onto a single image to check the distortion of its distribution. We observed that, the outputs generated by the algorithms are quite dispersed and deviated from the manually selected macula center. In Figure 5a, the Gaussian kernel density estimation of the MI [12] algorithm outputs is shown for the macula and of the ODfv [10] algorithm for the OD, respectively. Therefore, we propose to compute the distortion in the data and applying a shift operation prior to actual combination of outputs for finding macula center to make the individual algorithms unbiased. To compute the shift factor we calculate the average difference between the candidate of the algorithm and the manually selected macula center for those n images, where the algorithm successfully found the macula/OD region. That is, for the horizontal and vertical components of the shifting vector we have:

$$dx = \sum_{i=1}^{n}(x_i - x_{mi})/n \quad , \quad dy = \sum_{i=1}^{n}(y_i - y_{mi})/n \, ,$$

where $(\mathrm{x}_i, \mathrm{y}_i)$ stands for the fovea/OD center candidate of the algorithm on the i^{th} image, while $(\mathrm{x}_{mi}, \mathrm{y}_{mi})$ is for the manually selected fovea/OD center. The new outputs distribution is generated by applying the distortion shift factor on each output pixel coordinate.

3.2. OD and macula detection separately

3.2.1. Detecting hotspot region for OD/macula

We first devised a circular template voting scheme to determine the hotspot region i.e., an area in the image where majority of the outputs lies. A circular template of radius R is fit on each pixel in the image and outputs of candidate algorithms that fall within the radius of the predefined circular template are counted. Following the principal of majority voting, the center of the circular templates covering the maximum number of OD detectors and macula detector outputs in its radius is

considered to be the OD and macula hotspots, respectively. There can be more hot spots covering the maximum number of detector outputs in their radius; hence they together define a hot spot region, the patch with highest probability. The radius R of the template was set to 102 pixels, keeping in view the fact that clinically this is the average OD radius at the investigated resolution (field of view FOV equal to 1432). If there is a tie then such conflict are handled using an additional post processing e.g., for OD detection, the Gaussian filter is applied on the green channel of the image with a large sigma ($\sigma = 300$). The smoothened image is then subtracted from the original image to get resultant image, a rather darker image in which OD appears as a brighter patch as compare to the background image. The average intensity around the detectors outputs is computed using the same circular template, and the template with the highest average intensity is selected as the best OD hotspot region. In case of macula detection, we observed and tested that the vessel based macula detection algorithm M_{ta}[1] influenced the combination result therefore whenever there is conflicting situation or ties among hotspot regions, the hotspot region containing algorithm M_{ta} output is given preference and is selected for further processing. If the output of M_{ta} is lying isolated and not as part of any hotspot regions detected, then such conflicting situation is handled by computing distance between hotspots centers and the center of the image followed by selecting the minimum distanced region.

3.2.2. Center of the Hotspot based on a weighted combination

The center of the final hotspot regions could be found by averaging algorithms outputs, however, for a more accurate estimation, weights $w_i$can be computed for the x-coordinates and y-coordinates of the detectors outputs. If we denote the output centers of the individual algorithms by random variables $S_1(x_1, y_1)$, $S_2(x_2, y_2)$,...,$S_N(x_N, y_N)$ with distinct variances $Var(S_i) = \sigma_i^2 > 0$,then the problem of outputs combination is to reduce these N outputs to one final center $S_w(x_w, y_w)$. An appropriate combination of the outputs can be the weighted linear combination

$$S_w = \sum_{i=1}^{N} w_i S_i, \tag{1}$$

where $w_1, w_2, \ldots, w_N$ are non-negative weights, constrained to sum to 1. This constraint guarantees the combined estimate to remain unbiased. The variance of the estimator S_w is determined by the choice of weights and the variances of the individual outputs. When the random variables are independent then the variance of the estimator $S_w$is determined only by the choice of weights and the variance of individual outputs. In this case we have to minimize the expression below

$$Var(S_w) = \sum_{i=1}^{n} w_i^2 \, Var(S_i). \tag{2}$$

In this way the choice of weights that minimize the variance of the combined estimate is

$$w_i = \sigma_i^{-2} \Big/ \sum_{j=1}^{n} \sigma_j^{-2}$$

as a result of [15]. Choosing these weights leads to small variance, hence, the expected Euclidean distance from the true center of the combined estimate can be minimized. The higher the weight for an output, the more that detector is trusted to provide the correct answer. In the other case, when the random variables are dependent then we have to consider the pair wise covariances, as well.

4. Results and discussion

We have evaluated our proposed combination of algorithms to localize optic disc and macula on the publically available three databases: Diaretdb0 [16], Diaretdb1 [17] and DRIVE [18].

4.1. Optic disc detection results

The methods have been evaluated on the basis of two criterions i.e., to fall inside the manually selected optic disc patches and to be close to the manually selected OD center. Table 1 shows the correct detection of the OD location based on optic disc patch; the percentage detection rate of the proposed approach is higher than any of the individual algorithms. In Table 2 we can see the secondary error term that measures the average Euclidean distance of the candidates from the manually selected OD centers. We can observe that the combined system led to more accurate center localization than any of the individual algorithms.

TABLE I.
CANDIDATES FALLING INSIDE MANUALLY SELECTED OD PATCH.

	Optic Disc detector algorithms					
Test databases	OD_{pd}	OD_{ed}	OD_{fv}	OD_{ef}	OD_{ht}	**Combined system**
Diaretdb0	89%	76%	79%	94%	75%	**96%**
Diaretdb1	88%	77%	78%	96%	79%	**97%**
Drive	84%	98%	80%	98%	84%	**100%**
Total average	**88%**	**81%**	**79%**	**95%**	**78%**	**97%**

TABLE II.
AVERAGE EUCLIDEAN ERROR OF THE OD CANDIDATES.

	Optic Disc detector algorithms					
Test databases	OD_{pd}	OD_{ed}	OD_{fv}	OD_{ef}	OD_{ht}	**Combined system**
Diaretdb0	38.70	51.00	42.19	26.43	23.86	**15.84**
Diaretdb1	37.44	54.35	50.77	28.38	25.07	**17.54**
Drive	45.57	17.38	52.92	27.51	24.23	**15.02**
Total average	**39.80**	**44.74**	**47.25**	**27.29**	**24.33**	**16.10**

4.2. Macula detection results

The methods have been evaluated on the basis of two criterions i.e., macula error and fovea error. The macula error is the number of times the algorithm's output falls within the 0.5 DD radius of the manually selected macula center (Table 3), and fovea error i.e., the average Euclidean distance of these candidates and the manually selected centers (see Table 4). Results are given in pixels at the resolution of ROI diameter = 1432 (average ROI diameter of Diaretdb0 and Diaretdb01). Just

like the OD, the combined system provided more accurate results than any of the individual algorithms both for the primary error and secondary error terms.

TABLE III
CANDIDATES FALLING IN MACULA REGION.

	Fovea detector algorithms					
est databases	M_I	M_{sr}	M_{ta}	M_n	M_{wm}	**Combined system**
Diaretdb0	68%	72%	85%	86%	63%	**94%**
Diaretdb1	62%	76%	79%	92%	71%	**100%**
Drive	66%	76%	53%	68%	82%	**85%**
Total average	**66%**	**74%**	**77%**	**85%**	**69%**	**95%**

TABLE IV.
AVERAGE EUCLIDEAN ERROR OF THE FOVEA CANDIDATES.

	Fovea detector algorithms					
est databases	M_I	M_{sr}	M_{ta}	M_n	M_{wm}	**Combined system**
Diaretdb0	26.59	26.85	37.82	25.34	24.11	**20.19**
Diaretdb1	26.32	27.45	35.67	26.80	24.77	**19.68**
Drive	18.15	26.20	37.29	37.77	20.85	**16.24**
Total average	**25.22**	**26.95**	**37.04**	**27.71**	**23.83**	**19.42**

References

[1] A. D. Fleming, S. Philip, K. A. Goatman, J. A. Olson, and P.F. Sharp, "Automated Assessment of Diabetic Retinal Image Quality Based on Clarity and Field Definition", Investigative Ophthalmology and Visual Science, 47, pp. 1120-1125, 2006.

[2] C. Mariño, S. Pena, M. G. Penedo, J. Rouco, J. M. Barja, "Macula precise localization using digital retinal angiographies", Proceedings of the 11th WSEAS International Conference on Computers, Agios Nikolaos, Greece, pp. 601-607, 2007.

[3] S. Sekhar, W. Al-Nuaimy, A. K. Nandi, "Automated localization of optic disc and fovea in retinal fundus images", 16^{th} European Signal Processing Conference, Lausanne, Switzerland, 5 pages, 2008.

[4] F. Mendels, C. Heneghan, and J. P. Thiran, "Identification of the Optic Disk Boundary in Retinal Images using Active Contours", in Proc. Irish Machine Vision Image Processing Conf, pp. 103–115, Sept. 1999.

[5] S. Sekhar, W. Al-Nuaimy, and A. Nandi, "Automated Localisation of Retinal Optic Disk using Hough Transform", in Proccedings of the 5th IEEE International Symposium on Biomedical Imaging: From Nano to Macro, ISBI 2008, pp. 1577–1580, Paris, 2008.

[6] Lalonde, M., Beaulieu, M. and Gagnon, L., "Fast and Robust Optic Disk Detection using Pyramidal Decomposition and Hausdorff-Based Template Matching", IEEE Trans. Medical Imaging, vol. 20, pp. 1193-1200, Nov. 2001.

[7] Sopharak, A., Thet New, K., Aye Moe, Y., N. Dailey, M., Uyyanonvara, B., "Automatic Exudate Detection with a Naive Bayes Classifier", International Conference on Embedded Systems and Intelligent Technology, Grand Mercure Fortune Hotel, Bangkok, Thailand, pp. 139–142, 2008.

[8] N. Otsu, "A Threshold Selection Method from Gray-Level Histograms", IEEE Trans. Syst. Man and Cybern. pp. 62-66, 1979.

[9] S. Ravishankar, A. Jain, A. Mittal, "Automated Feature Extraction for Early Detection of Diabetic Retinopathy in Fundus Images", CVPR - IEEE Conference on Computer Vision and Pattern Recognition, pp. 210-217, 2009.

[10] M. Niemeijer, M. D. Abrŕmoff , B. van Ginneken, "Fast detection of the optic disc and fovea in color fundus photographs", Medical Image Analysis, vol. 13, pp. 859–870, 2009.

[11] M. Niemeijer, J.J. Staal, B. van Ginneken, M. Loog, M.D. Abramoff, "Comparative study of retinal vessel segmentation methods on a new publicly available database", in: SPIE Medical Imaging, Editor(s): J. Michael Fitzpatrick, M. Sonka, SPIE, 2004, vol. 5370, pp. 648-656.

[12] T. Petsatodis, A. Diamantis, G.P. Syrcos. "A Complete Algorithm for Automatic Human Recognition based on Retina Vascular Network Characteristics", 1st International Scientific Conference e RA, Tripolis, Greece, pp. 41-46, 2004.

[13] F. Zana , I. Meunier , J. C. Klein, "A region merging algorithm using mathematical morphology: application to macula detection", Proceedings of the fourth international symposium on Mathematical morphology and its applications to image and signal processing, Amsterdam, The Netherlands, pp. 423 - 430, 1998.

[14] Dietterich T. G., "Ensemble Methods in Machine Learning", Multiple Classifier Systems, LNCS, vol. 1857/2000, pp. 1-15, 2008

[15] W. G. Cochran, "Problems arising in the analysis of a series of similar experiments", Journal of the Royal Statistical Society, 4(Suppl.), pp. 102–118, 1937.

[16] T. Kauppi, V. Kalesnykiene, J.K. Kamarainen, L. Lensu, I. Sorri, H. Uusitalo, H. Kalviainen, J. Pietila: "Diaretdb0: Evaluation database and methodology for diabetic retinopathy algorithms", Technical report, Lappeenranta University of Technology, Lappeenranta, Finland, 2006.

[17] T. Kauppi, V. Kalesnykiene, J.K. Kamarainen, L. Lensu, I. Sorri, A. Raninen, R. Voutilainen, J. Pietilä, H. Kälviäinen, H. Uusitalo: "DIARETDB1 diabetic retinopathy database and evaluation protocol", In Proc. of the Medical Image Understanding and Analysis, Aberystwyth, UK, pp. 61–65, 2007.

[18] J. J. Staal, M. D. Abramoff, M. Niemeijer, M. A. Viergever, and B. van Ginneken, "Ridge Based Vessel Segmentation in Color Images of the Retina", IEEE Transactions on Medical Imaging, vol. 23, pp. 501–509, 2004.